Available online at www.sciencedirect.com
SCIENCE DIRECT
Thermochimica Acta 445 (2006) 126–132
thermochimica acta
www.elsevier.com/locate/tca

Heat conduction effects during the calorimetric determination of absorbed dose to water in radiotherapy beams

A. Krauss *

Physikalisch-Technische Bundesanstalt (PTB), Bundesallee 100, D-38116 Braunschweig, Germany

Available online 30 September 2005

Abstract

A transportable water calorimeter for the determination of the quantity of absorbed dose to water in radiotherapy beams has been developed at the PTB and is presented in detail in this investigation. Heat conduction effects occurring in the calorimeter are studied for different lateral sizes of high-energy photon beams, for different depth dose distributions of electron beams and for a scanned-beam irradiation with a heavy ion beam. The corresponding correction factors are calculated and arguments are given under which conditions these can adequately be applied.

Keywords: Absorbed dose to water; Transportable calorimeter; Heat conduction calculation; Radiotherapy beams; Scanned-beam

1. Introduction

The quantity of absorbed dose to water, D_w, is the measurement in the dosimetry for radiation therapy and can be determined most directly with the aid of a water calorimeter [1,2] by measuring the radiation-induced temperature rise, $\Delta\vartheta$, at a point in a water phantom:

$$D_w = \Delta\vartheta c_p (1-h)^{-1} \Pi k_i \quad (1)$$

To achieve a high accuracy of measurement, several influence quantities affecting the temperature measurement have to be considered, for example the so-called heat defect, h, which is a possible difference between the energy imparted to water and the energy occurring as heat [3,4], or different heat conduction effects due to the absorption of the radiation. In Eq. (1) the heat conduction corrections, k_C, as well as further corrections are combined to the product Πk_i.

At the Physikalisch-Technische Bundesanstalt (PTB) a water calorimeter is implemented as the primary standard for realizing the unit gray (Gy) of absorbed dose to water for ^{60}Co-radiation with a relative standard uncertainty of less than 0.3% [5]. Based on PTB's primary standard water calorimeter different devices such as ionization chambers, for example, which are routinely used for basic dosimetric measurements in hospitals, are calibrated in terms of absorbed dose to water under reference conditions. Following the reference conditions in the case of ^{60}Co-radiation, the point of measurement is located at the central axis of an extended radiation beam of 10 cm × 10 cm in a depth of 5 cm inside a water phantom of 30 cm edge length, which is placed in a distance of 95 cm to the ^{60}Co-source [6]. For this condition, the dose gradients in the vicinity of the point of measurement inside the water phantom of the calorimeter are small enough, that the corrections for heat conduction effects caused by these dose gradients are almost negligible.

However, new applications in radiation therapy with high-energy photon and electron radiations, and furthermore also with ion beams like protons or carbon ions, make use of much smaller lateral field sizes than those mentioned above. The reasonable use of a water calorimeter for these non-reference conditions may be limited by the much stronger heat conduction effects occurring in these cases. Nevertheless, the calorimetric determination of the quantity of absorbed dose to water in radiotherapy beams is of great interest, as it is the most direct method to achieve the quantity in absolute terms. At PTB, an additional calorimeter, based on the initial

* Tel.: +49 531 5926230.
E-mail address: achim.krauss@ptb.de.

0040-6031/$ – see front matter © 2005 Elsevier B.V. All rights reserved.
doi:10.1016/j.tca.2005.08.016

design by Pieksma et al. [7] has been developed besides the above-mentioned primary standard water calorimeter, which can be used as a transportable device applicable not only at a standard laboratory but also at a radiation therapy facility.

In this paper, the transportable water calorimeter will be presented in detail and it will be discussed how far the water calorimeter can be used in radiotherapy beams without increasing the measurement uncertainty excessively. By means of heat conduction calculations on the basis of the finite-element-method, correction factors for the calorimetric determination of absorbed dose to water are calculated for radiation beams of different lateral extensions as well as for the special case of irradiations with a heavy ion beam using the so-called scanned-beam or raster-scan method. Additionally, heat conduction effects are investigated which occur due to the temperature gradients caused by different depth dose distributions in water, for instance for electron radiation of different energy.

2. Material and methods

2.1. Calorimeter

The PTB primary standard water calorimeter as well as the new transportable calorimeter mainly use identical components as, for example, the water phantom and the calorimetric detector, which have been described in previous publications [8,9]. Briefly, a water calorimeter consists of a water-filled cubic phantom of 30 cm edge length, made of 1 cm thick polymethylacrylate (PMMA) walls. The horizontally directed radiation enters the phantom through a 3 mm thick PMMA window. As the calorimeter is operated at a water temperature of 4 °C to avoid convection inside the water phantom, and as the radiation-induced temperature increase to be measured amounts to only about 0.24 mK/Gy, the phantom of the calorimeter is thermally isolated by a layer of polystyrene, several centimetre thick, surrounded by an active temperature stabilization system.

The method of temperature stabilization of the transportable calorimeter significantly differs from that used in the primary standard calorimeter and is realized by a sandwich structure made of 11 mm thick, actively cooled aluminium plates fixed between two 5 cm thick layers of polystyrene. The six sides of the water phantom are completely covered by this structure, leaving open only the 12 cm × 12 cm radiation entrance window where the thickness of the polystyrene layer, shielding the water phantom from room temperature, amounts to 15 cm. That cooling plate, which is located at the top side, is machined as a traversable lid to enable access to the water phantom. In detail, each plate consists of a lower plate, 9 mm in thickness, in which a cooling channel with a rectangular cross-section of 7 mm × 10 mm has been milled out in a meander-like structure (Fig. 1), and a cover plate, 2 mm in thickness, to seal the channel. The cooling channels are connected in parallel to an outside cooling unit which

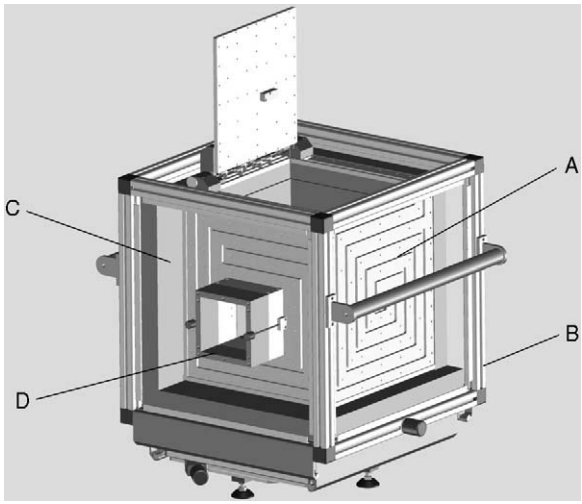

Fig. 1. Constructional drawing of the transportable calorimeter, showing the cooling plates with the meander-like channels (A), the outer frame structure (B), parts of the polystyrene shielding (C) and the radiation entrance window (D).

is suited to fix the temperature of the cooling plates to better than ±0.01 °C. The external Pt-100 sensor of the cooling unit is placed at the surface of one of the aluminium plates. Additional Pt-100 sensors placed on each plate are used to monitor their temperatures during the operation of the calorimeter. Fig. 2 shows a picture of the transportable water calorimeter, which has an almost cubic shape of about 60 cm edge length.

When the calorimeter is put into operation, the cooling liquid does not only flow through the channels inside the aluminium plates but is by-passed to a stainless steel tube located inside the water phantom. The water inside the phantom is permanently mixed by means of a magnetically coupled stirrer located at the bottom of the phantom. To accelerate the cooling procedure, the temperature of the cooler is first set to 2.5 °C, which decreases the temperature of the water in

Fig. 2. Picture of the transportable water calorimeter with the corresponding cooling unit. The calorimeter has an almost cubic shape of about 60 cm edge length.

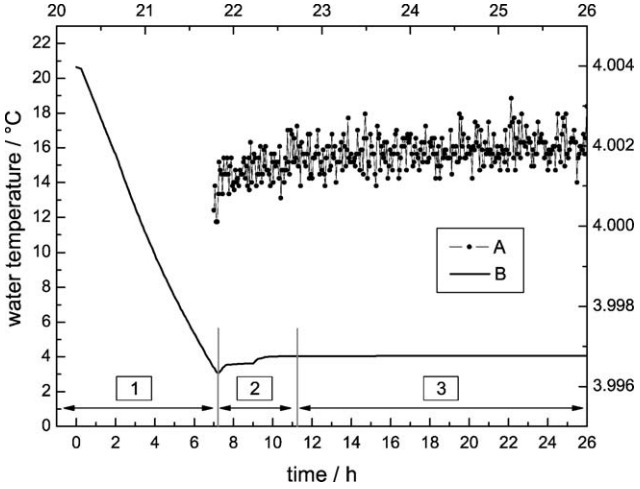

Fig. 3. Water temperature (B) in the calorimeter during the cooling procedure. The set-point of the cooler is changed from 2.5 to 4 °C at the end of time interval (1). During interval (2), the water temperature is heated up to 4 °C step by step and remains unchanged during the period that follows (3). By means of the upper time scale and the right temperature scale of the graph, the water temperature (A) is shown in an expanded view for a part of the time period (3).

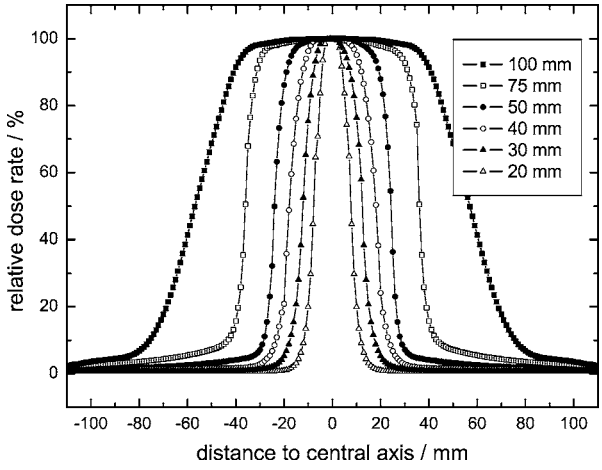

Fig. 4. Lateral dose distributions for high-energy photon radiation beams of different field sizes. The curves shown are based on measurements performed at the linear accelerator of the PTB for field sizes between 20 and 75 mm and at the ^{60}Co-source for a field size of 100 mm, respectively.

the phantom to about 3.5 °C after about 7 h. Then the cooling bypass into the phantom is switched off and the set-point for the cooler temperature is increased to 4 °C, followed by a step-by-step procedure in which the water temperature is slowly heated up to 4 °C by means of a heating wire which surrounds the above-mentioned stainless steel tube inside the phantom. After that, the stirrer in the phantom is switched off. The whole cooling procedure is completely automated and takes typically 18–24 h before the remaining temperature gradients in the calorimeter are low enough for irradiation measurements to be started (Fig. 3).

The calorimetric detector [9] consists of a plane-parallel glass cylinder filled with high-purity water, in which two thin cone-shaped glass pipettes are mounted perpendicular to the cylinder axis and opposite each other, such that the opposing tips of the pipettes are separated by about 8 mm. The tip of each pipette contains a thermistor sensor 0.25 mm in diameter. The detector can be fixed at different water depths in relation to the entrance window of the phantom and is mounted such that the axis of the radiation field coincides with the cylinder axis.

2.2. Heat transport calculations

When the water calorimeter is applied for measurements in an extended radiation field, the dominant heat conduction effects arise due to the irradiation of the non-water materials of the detector (e.g. glass), because the values of the specific heat capacities and of the radiation interaction coefficients of these materials deviate from those of water. The corresponding corrections for these effects for ^{60}Co-radiation have been extensively studied in previous publications [9,10]. For the present investigation, the additional heat conduction effects caused by irradiations with smaller lateral field sizes as well as for different depth dose distributions have been calculated. A two-dimensional model of the water phantom without the detector was used within a finite-element programme (ANSYS 7.1). The element size of the model was chosen to be 1 mm × 1 mm. The transient calculations for this investigation were performed for an irradiation time of 120 s, followed by a drift period without radiation of the same duration. This corresponds to the standard operating mode of the water calorimeter.

Most of the heat generation rates used in the calculations were derived from experimentally determined dose distributions measured at the PTB linear accelerator or at the ^{60}Co-source, respectively. The measurements were performed in a water phantom by the help of a small ionization chamber fixed in a PMMA mount which could be automatically moved either in horizontal and vertical direction in respect to the mid-axis of the field or in parallel to the direction of the radiation. To generate mathematical expressions for the heat generation rates applicable within the finite-element programme, the measured distributions were fitted by combinations of polynomial and exponential functions. Fig. 4 presents these curves for photon radiation beams with different lateral dose distributions having full width at half maximum-value (fwhm) ranging from 20 to 100 mm. For electron and photon radiations of different energies, depth dose distributions in the direction of the radiation were measured at the central axis of the radiation beam. Fig. 6 shows the principal functional dependence of the corresponding heat generation rates for these cases and for the case of a 300 MeV carbon ion beam. For the study of the heat conduction effects occurring in irradiations using the scanned-beam method, the heat generation rates for the calculations were derived from the assumed Gaussian-shaped intensity distribution of the carbon ion beam with an fwhm-value of 6 mm.

3. Results and discussion

In this section, correction factors are presented for the calorimetric determination of absorbed dose to water according Eq. (1). The heat conduction corrections, k_C, are based on the results of finite-element heat conduction calculations and are defined as the ratio of a calorimetric result without and with influence of the heat conduction effects. The adequate application of the corrections requires that the experimental value and the calculated correction have been determined for the same case, that means identical time intervals must be used for the linear extrapolations of the pre- and post-irradiation drift curve to the mid-run position. For an irradiation time of 120 s, these time intervals are 110 s each for the pre- and post-irradiation drift curve, with the latter one starting 10 s after the end of the irradiation [9].

3.1. Lateral dose distributions

The correction factor, k_C, for the heat conduction effects caused by the limited size of the radiation beams has been calculated in dependence of the field size for different lateral positions in respect to the central axis of the fields. This reflects the fact that the two thermistors of the calorimetric detector are both about 4 mm separated from the central axis. For this point of measurement, an additional correction factor, k_R, which is given by the ratio of the dose rate at the central axis of the beam to the dose rate at the point of measurement, has to be applied to obtain the absorbed dose to water under reference conditions. The conductive corrections, k_C, for the case of an irradiation time of 120 s and the non-conductive corrections, k_R, are shown in Fig. 5. Both relative corrections are below 0.5% for field sizes larger than

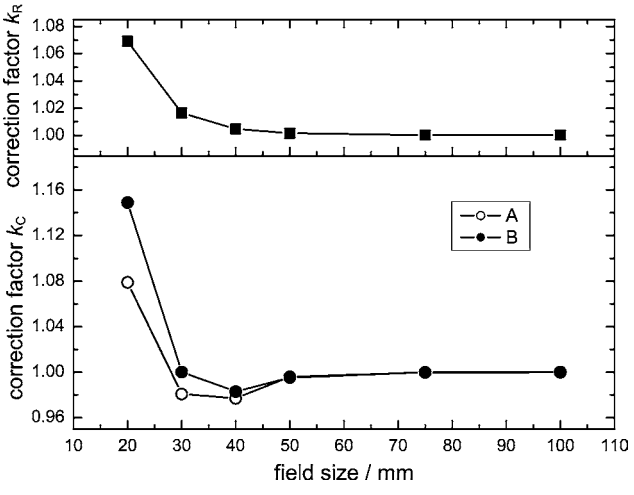

Fig. 5. Calculated correction factor k_C and k_R (upper part of the graph) for an irradiation time of 120 s as a function of the field size. The correction k_R corrects for the dose rate difference between the central axis of the radiation beam and the point of the caloric measurement, which is 4 mm away from the central axis. The correction k_C corrects for the heat conduction effects due to the lateral dose distribution and is given for the point of the caloric measurement (B) as well as for the central axis of the radiation beam (A).

50 mm × 50 mm, but for smaller field sizes the corrections increase. For instance, the conductive correction k_C for the point of measurement being 4 mm away from the central axis already amounts to about 0.983 for a field 40 mm × 40 mm in size. Furthermore it can be seen that for even smaller field sizes there is a strong variation in the amount and also in the direction of the correction. This is an indication that for the smaller field sizes, the corrections start to depend sensitively on a precise knowledge of the shape and width of the dose distribution and of the position of the measurement, respectively. The question arises if the correction factors k_C and k_R can be adequately applied for these irradiation conditions or, in other words, which standard uncertainties can be assigned to the corrections.

From additional finite-element calculations simulating possible variations of the width of the dose distributions by about ±1 mm, which may be caused by instabilities of the accelerator during the caloric measurements, the standard uncertainty of the heat conduction correction k_C is estimated to be about ±0.002 for a field size of 40 mm × 40 mm and about ±0.018 for a field size of 20 mm × 20 mm. Furthermore, also the symmetry (“flatness”) of the radiation beam in respect to the central axis is very likely to change during the caloric measurements, which probably causes an additional uncertainty of at least the same amount as given above. At the same time the conductive correction factor k_C varies due to instabilities of the lateral dose distribution, also the non-conductive correction factor k_R changes. Although the position of the thermistors inside the calorimetric detector is precisely known within an uncertainty of 0.1 mm, a change in the shape of the dose distribution can be regarded as a hypothetical change of the point of measurement in respect to the central axis of the field. Therefore, for an estimate of the uncertainties of the non-conductive correction factor k_R, the point of measurement is assumed to also vary within ±1 mm for a given lateral dose distribution. This way, the standard uncertainty of the correction k_R in the case of the 40 mm × 40 mm and the 20 mm × 20 mm field amounts to ±0.002 and ±0.074, respectively.

Although smaller correction factors can be achieved for shorter irradiation times, it must be concluded that the use of a water calorimeter of the given design may be generally limited to radiation beams with a geometric width greater than 40 mm. For these cases, the calorimetric determination of absorbed dose to water within a relative combined standard uncertainty of less than 1% is achievable if it is assumed that corrections for other influence quantities, which are not being dealt with in this investigation, remain unchanged for the different beams. Clearly the results presented in this section depend on the individual width and shape of the dose distributions available at the PTB. This can be different at other radiation facilities. Therefore, it is essential in any case to have a good knowledge of the lateral dose distribution and its stability over the time of the calorimetric measurements in order to be able to calculate the correction factors properly.

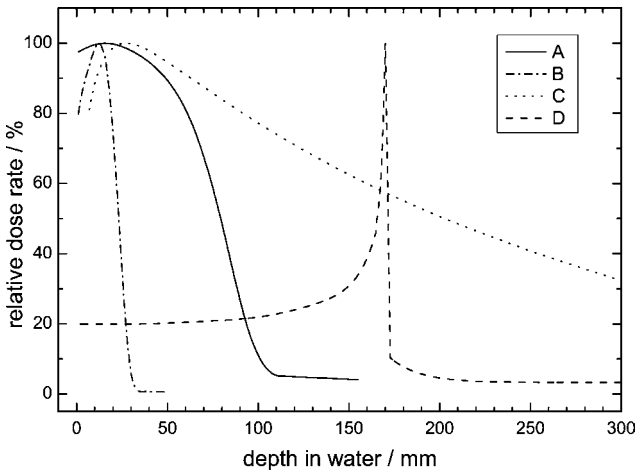

Fig. 6. Depth dose distributions in water for 20 and 6 MeV-electron radiation (A and B) and for 16 MV photon radiation (C), based on measurements performed at the linear accelerator of the PTB. In case of the 300 MeV carbon ion beam (D) only the principal shape of the distribution is shown.

3.2. Depth dose distributions

From Fig. 6 it can be expected that the influence of heat conduction effects driven by the depth dose distribution will be very small for photon radiation as the dose gradients are generally small. Corresponding heat transport calculations have been performed for ^{60}Co-, 8 MV-, and 16 MV-photon radiation. In all cases, the conductive correction factor for an irradiation time of 120 s is less than 0.01% at the reference point of measurement, which is in a water depth of 50 and 100 mm for ^{60}Co- and high-energy photon radiation, respectively [6]. This principally differs from the case of high-energy electron or ion beams. For these types of irradiation, large temperature gradients caused by the depth dose curves (Fig. 6) occur in the water calorimeter. In case of the 6 and 20 MeV-electron depth dose distributions the correction factor k_C at different water depths is given in Table 1, which reflects the fact that the measurements can be performed at different reference points, following either the recommendations of the IAEA- or of the DIN-dosimetry protocol [6,11]. It can be seen that the calculated corrections amount to less than 1% and more than 4% in case of the 20 and 6 MeV-electron radiation at 20 mm depth in water, respectively. However, for the transportable water calorimeter presented in this investigation, the remaining temperature drift without irradiation at a water depth smaller than or equal to 20 mm is still affected by the influence of the room temperature outside the calorimeter. During irradiation, this additional drift is superimposed by the depth dose driven temperature drifts and may result in unpredictable corrections. It must be concluded that the use of the water calorimeter in electron radiation is limited to energies higher than about 13 MeV, for which the recommended point of measurement according the IAEA-protocol is at a water depth beyond 30 mm. For these cases, the standard uncertainties of the calculated correction factors k_C are smaller than $\pm 5 \times 10^{-4}$, considering small variations in the finite-element-model as well as in the mathematical expressions for the heat generation rates used in the calculations.

Table 1
Heat conduction effect caused by different electron depth dose distributions

MeV	z^a (mm)	k_C	z^b (mm)	k_C
6	20.0	1.0423	13.7	1.0396
20	20.0	1.0066	47.8	0.9999

Correction factor k_C at different water depths z.
[a] Depth recommended by DIN [11].
[b] Depth recommended by IAEA [6].

The very large temperature gradients in the vicinity of the maximum of the depth dose curve of the 300 MeV-carbon beam are by far too large for any direct calorimetric determination of absorbed dose to water at that point. However, in the clinical application of this type of radiation, the beam energy is varied within a certain range to achieve a depth dose distribution offering a narrow plateau region with an almost constant dose rate. In this case, depending on the width of the plateau region, similar heat conduction corrections as discussed in Section 3.1 could be expected if the measurements could be performed in a quasi-static radiation field, i.e. the variation of the energy must be done fast enough, that heat conduction effects due to the superposition of the depth dose curves of the single beams can be neglected. Otherwise the measurements with the calorimeter should be performed using a radiation beam of constant energy and the point of measurement should be chosen to be at the smooth part of the dose distribution in a water depth between 50 and 100 mm. In this case the conductive corrections caused by the depth dose distribution are negligible.

3.3. Scanned-beam

In radiotherapy treatments with proton or heavy ion beams using the scanned-beam method, a radiation beam with a pencil-like lateral dose distribution is moved step by step across the desired area in less than 1 min. By simultaneously varying the dose rate and energy of the beam during the scanning procedure, the whole tumour volume can be irradiated with the prescribed dose. However, for a calorimetric determination of absorbed dose to water it may be more adequate to use a constant dose rate as well as a constant energy (see Section 3.2) throughout the measurement. This way, depending on the step size during the scanning procedure, an almost homogeneous lateral dose distribution is achieved towards the end of the scan. The time evolution of the corresponding temperature distribution in water, which arises from the superposition of the single beams, is mainly determined by the irradiation time at each position of the scanned area.

To investigate the heat conduction effects in case of the scanned-beam method, finite-element calculations were performed for an irradiation with a 300 MeV carbon beam having an fwhm of 6 mm, which is scanned across an area of 52 mm × 52 mm using a step size of 4 mm. This results in variations of the lateral dose distribution of only about 0.04%.

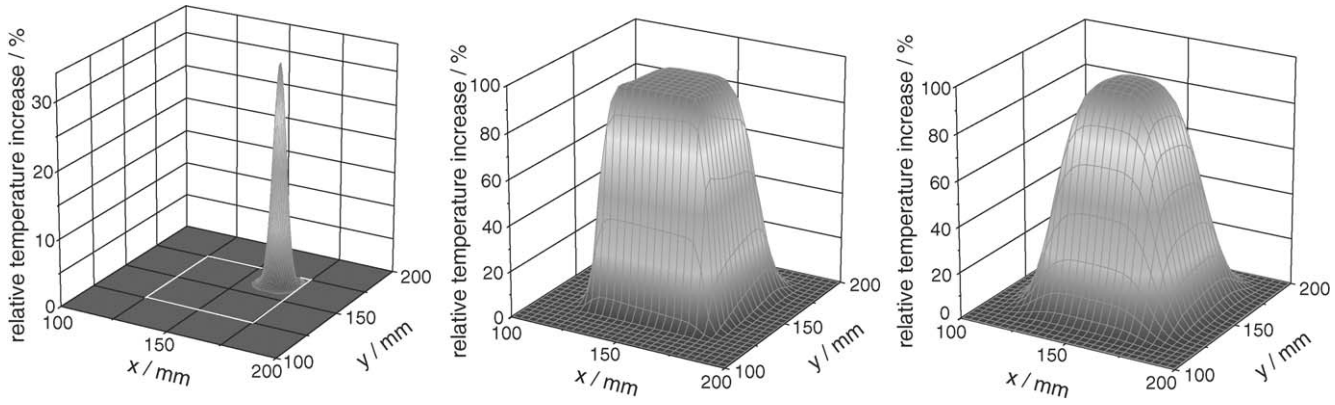

Fig. 7. Calculated three-dimensional temperature distributions in case of the scanned-beam method. A 300 MeV carbon ion beam with an fwhm-value of 6 mm (left part) is scanned across an area of 52 mm × 52 mm with a step size of 4 mm. The irradiation time for each step is 0.1 s. The middle and the right part of the figure show the temperature distributions at the end of the seven times repeated scan and 120 s after the end of the scan, respectively.

The irradiation time at each of the 169 beam positions is assumed to be 0.7 s. Additionally, a seven times repeated scan was studied by using a single irradiation time of 0.1 s and the same scan-parameter as mentioned above. The total irradiation time is about 118 s in this case, which is comparable to other irradiation conditions used in the present investigation. The calculated three-dimensional temperature distributions at the beginning of the first scan, at the end of the seventh scan and 2 min after the end of the irradiation are shown in Fig. 7. From the middle part of the figure it can be seen that at the end of the irradiation the temperature at the plateau region of the distribution is nearly constant, offering only a small increase to those positions of the scanned area, which have been irradiated at last. Based on such temperature distributions, the conductive correction factor k_C for the calorimetric determination of absorbed dose to water is calculated to be 0.9992 and 0.9982 for the single scan at the central axis of the field and 4 mm apart the axis, respectively. In case of the seven times repeated scan, the corrections are nearly the same and amount to 0.9990 and 0.9981 at the central axis and 4 mm away from it, respectively. The standard uncertainty of the given correction due to possible variations in the finite-element calculations is smaller than $\pm 5 \times 10^{-4}$.

The investigation in this section shows that on principle, the water calorimeter is applicable for irradiations using the scanned-beam method. However, it should be accepted that the conductive corrections given here are only valid for the somewhat ideal situation of the calculations. In reality it has to be expected that the dose distribution of a single scan may not as homogeneous as assumed, which will strongly affect the heat conduction corrections.

4. Conclusions

The application of the transportable water calorimeter for the determination of absorbed dose to water in radiotherapy beams is limited to certain irradiation conditions. Heat conduction calculations for the case of an irradiation time of 120 s show that the geometric width of the radiation beam should be generally larger than 40 mm × 40 mm to keep the combined standard uncertainty for the determination of absorbed dose to water at less than 1%. When the transportable calorimeter is to be used for electron beams, a reasonable correction of the heat conduction effects caused by the depth dose distribution seems to be possible only for electron energies above 13 MeV. Furthermore it can be concluded that the irradiation conditions in case of the scanned-beam method with proton or heavy ion beams of constant energy can be adequately chosen for the use of a water calorimeter. Heat conduction calculations for the scanned-beam method investigating the combined effect of simultaneously varying the lateral position of the beam as well as the energy of the beam will be performed shortly.

For the transportable calorimeter presented in this investigation a further correction has to be applied for the so-called perturbation effect. Due to the aluminium cooling plates surrounding the calorimeter, the radiation field at the point of measurement will be disturbed to some extent. Preliminary results for ^{60}Co-γ-radiation predict this effect to amount to about 0.3%. In the near future the corresponding corrections for different kinds of radiation beams will be determined by the help of Monte-Carlo calculations as well as by comparative measurements with the primary standard water calorimeter.

References

[1] S.R. Domen, An absorbed dose water calorimeter: theory, design and performance, J. Res. Nat. Bur. Stand. 87 (1982) 211–235.
[2] C.K. Ross, N.V. Klassen, Water calorimetry for radiation dosimetry, Phys. Med. Biol. 41 (1996) 1–29.
[3] N.V. Klassen, C.K. Ross, Water calorimetry: a correction to the heat defect calculations, J. Res. Natl. Inst. Stand. Technol. 107 (2002) 171–178.
[4] A. Krauss, H.-M. Kramer, The heat defect in the PTB water calorimeter: a discussion on uncertainty, in: Proceedings of the Work-

shop on Recent Advances in Absorbed Dose Standards, ARPANSA, Melbourne, 2003.
[5] A. Krauss, The future PTB primary standard for absorbed dose to water in ^{60}Co-radiation, in: Proceedings of the International Symposium on Standards and Codes of Practice in Medical Radiation Dosimetry, IAEA, 2003, pp. 75–82 (ISBN 92-0-111403-6).
[6] IAEA TRS 398, Absorbed dose determination in external beam radiotherapy: an international code of practice for dosimetry based on standards of absorbed dose to water, IAEA, Vienna, 2000 (ISBN 92-0-102200-X).
[7] M. Pieksma, L.A. De Prez, E. Van Dijk, A.H.L. Aalbers, Measurements of kQ beam quality correction factors for the NE 2611A chamber in high energy photon beams using the Nederlands Meetinstituut water calorimeter, in: Proceedings of the International Symposium on Standards and Codes of Practice in Medical Radiation Dosimetry, IAEA, 2003, pp. 93–103 (ISBN 92-0-111403-6).
[8] A. Krauss, M. Roos, The heat defect in the water absorbed dose calorimeter, Thermochim. Acta 229 (1993) 125–132.
[9] A. Krauss, Experimental verification of calculated radiation-induced heat conduction effects in the water absorbed dose calorimeter, Thermochim. Acta 382 (2002) 99–107.
[10] A. Krauss, M. Roos, Heat transport by material dependent heating during absorption of radiation in the water absorbed dose calorimeter, Thermochim. Acta 337 (1999) 45–49.
[11] DIN 6800-2, Dosismessverfahren nach der Sondenmethode für Photonen- und Elektronenstrahlung, Teil 2: Ionisationsdosimetrie, DIN, Berlin, 1997.